Electronic Supplementary Information

Defects as Catalytic Sites for Oxygen Evolution Reaction in Earth-Abundant MOF-74 Revealed by DFT

Jordi Morales-Vidal, Rodrigo García-Muelas, Manuel A. Ortuño*

Institute of Chemical Research of Catalonia (ICIQ) and Barcelona Institute of Science and Technology (BIST), Av. Països Catalans 16, 43007 Tarragona, Spain

E-mail: mortuno@iciq.es

Contents

1. Unit cell parameters

Table S1. Experimental X-ray and DFT computed lattice parameters for Co-MOF-74.

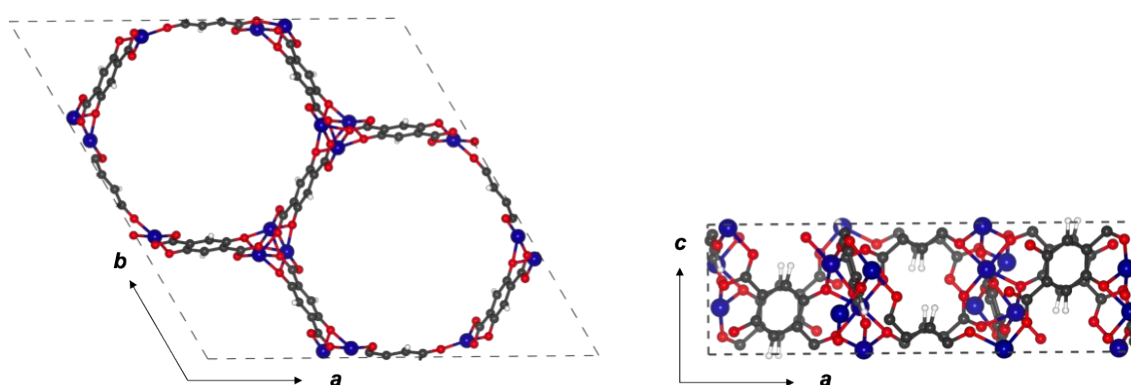| Unit cell	Lattice parameters (Å)		
	a	b	c
Experimental[1]	25.885	25.885	6.806
This work	26.129	26.129	6.821
Relative error (%)	0.94	0.94	0.22

Fig. S1 Top view (left) and side view (right) of Co-MOF-74 cell. Atom legend: M (blue), O (red), C (grey), and H (white).
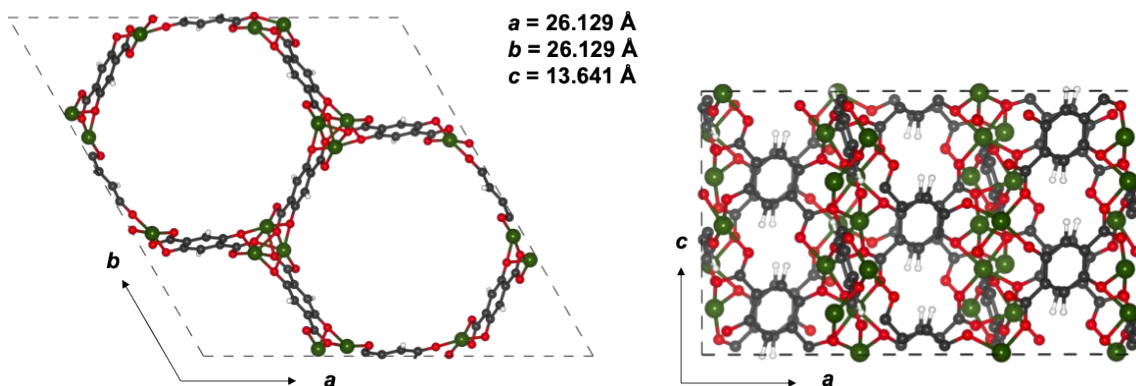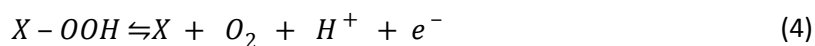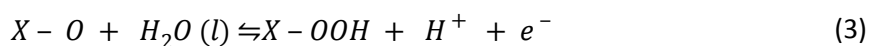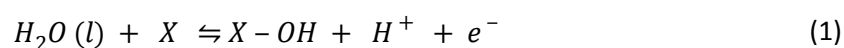
Fig. S2 Top view (left) and side view (right) of expanded Fe-MOF-74 cell. Atom legend: Fe (green), O (red), C (grey), and H (white).

2. Thermodynamics of OER

The water-nucleophilic attack (WNA) mechanism described in the main text has four reactions, Eq. 1-4. All of them occurs in solvated environment and contain a proton-coupled electron transfer (PCET). Therefore, their correct description in terms of Gibbs energies (*G*) requires corrections for (i) solvation, (ii) vibrational energies, and (iii) the computational hydrogen electrode. **X** represents any of the M-MOF-74 models and **X-OH**, **X-O**, and **X-OOH** correspond to hydroxo, oxo, and hydroperoxo intermediates (see main text). The kinetic energy barriers of such PCET steps are typically around 0.2 eV and can be considered surmountable at room temperature.[2]

$$H_2O\ (l)\ +\ X\ \leftrightharpoons X-OH\ +\ H^+\ +\ e^- \tag{1}$$

$$X-OH \leftrightharpoons X-O\ +\ H^+\ +\ e^- \tag{2}$$

$$X-O\ +\ H_2O\ (l) \leftrightharpoons X-OOH\ +\ H^+\ +\ e^- \tag{3}$$

$$X-OOH \leftrightharpoons X\ +\ O_2\ +\ H^+\ +\ e^- \tag{4}$$

The Gibbs energy (*G*) can be related to enthalpy (*H*) and entropy (*S*) through Eq. 5 and the *G* for each intermediate involved on the OER was obtained with Eq. 6. The enthalpy was approximated by adding vibrational energy corrections (E_{vib}) to the electronic DFT energy (E_{DFT}). E_{vib} was calculated from the computed normal modes of vibration (K) as showed in Eq. 7, where k_B is the Boltzmann's constant and Θ represents the characteristic vibrational temperature. The latest is defined as Eq. 8 which includes the Planck's constant (h) and the vibrational frequency for each normal mode (ν_K). Regarding the entropic term (*S*), it was

computed as the vibrational entropy (Eq. 9) for all intermediates but the values for H_2 and H_2O were taken from literature.[3]

$$G(T,p) = H(T,p) - TS(T,p) \tag{5}$$

$$G = E_{DFT} + E_{vib} - TS \tag{6}$$

$$E_{vib} = k_B \sum_K \frac{1}{2} \Theta_{v,K} \tag{7}$$

$$\Theta = \frac{h v_K}{k_B} \tag{8}$$

$$S = k_B \sum_K \left(\frac{\Theta_{v,K}/T}{e^{\Theta_{v,K}/T} - 1} - ln\left(1 - e^{-\Theta_{v,K}/T}\right) \right) \tag{9}$$

The potential energy of H^+ was obtained from the computational hydrogen electrode (CHE)[4] framework. The standard hydrogen electrode (SHE, pH = 0, p = 1 bar H_2, T = 298.15 K) at an electrode potential of u = 0 V vs SHE is taken as reference. Therefore, the electrons and solvated protons are considered to be in equilibrium with hydrogen in gas phase (Eq. 10). Thereby, the free energy of the proton can be written as one half of the Gibbs energy of $H_2(g)$ (Eq. 11). At different pH, a correction of $-k_B T \ln(10)pH$ is added to this potential energy. The $G_{H_2(g)}$ was obtained following Eq. 12, where $S_{H_2(g)}$ is taken from literature[3] as the experimental entropy of hydrogen in gas phase at standard conditions.

$$H^+_{(aq)} + e^- \leftrightharpoons \frac{1}{2}H_2(g) \tag{10}$$

$$\Delta G_{H^+} = \frac{1}{2}\Delta G_{H_2(g)} - k_B T \ln(10)pH \tag{11}$$

$$G_{H_2(g)} \approx E_{H_2(g),\ DFT} + E_{H_2(g),\ vib} - TS_{H_2(g)} \tag{12}$$

Similarly, the Gibbs energy (G) for liquid water, $E_{H_2O(l),DFT}$ was calculated by optimizing a water molecule in gas phase and adding a solvation correction computed with the implicit solvation model VASP-MGCM,[5] Eq. 13. The value of $S_{H_2O(l)}$ was also taken from literature.[3]

$$G_{H_2O\ (l)} = E_{H_2O(l),DFT} + E_{H_2O(g),\ vib} - TS_{H_2O(l)} \tag{13}$$

Finally, G_{O_2} was derived from the experimental Gibbs energy of water splitting as follows:

$$2H_2O\ (l) \leftrightharpoons 2H_2\ (g) + O_2\ (g) \quad \Delta G = 4.92\ eV \tag{14}$$
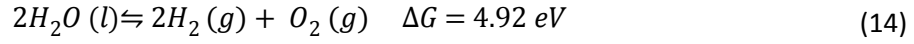
$$4.92\ eV = 2G_{H_2(g)} + G_{O_2} - 2G_{H_2O}\ (l) \tag{15}$$

$$G_{O_2} = 4.92\ eV + 2G_{H_2O}(l) - 2G_{H_2(g)} \tag{16}$$

The reaction energy ΔG for each step in the WNA mechanism can be expressed by Eq. 17, as all of them are PCET. The term $-|e|u$, which includes the charge of the electron (e) and the electrode potential (u), is added in order to account for a bias in the energy of the steps involving an electron when u is different to 0 V vs SHE. Eq. 17 was applied to each elementary step (Eq. 1–4) to produce Eq. 18-21. These are expressed in terms of DFT energies on Eq. 22-25. Eq. 18 and 22 represent the first reaction of the WNA mechanism (Eq. 1), which is the formation of the hydroxo intermediate (**X-OH**) with the release of one proton and one electron. The second PCET (Eq. 2) is the oxidation of **X-OH** to oxo (**X-O**) intermediate and is defined by Eq. 19 and 23. Eq. 20 and 24 represent the nucleophilic attack of a water molecule to **X-O** leading to hydroperoxo intermediate (**X-OOH**) and the release of one proton and one electron. The last PCET of the OER entails the formation of an oxygen molecule and is defined by Eq. 21 and 25.

$$\Delta G = \Delta E_{DFT} + \Delta E_{vib} - T\Delta S - k_B T \ln (10)pH - |e|u \tag{17}$$

$$\Delta G_1 = G_{X-OH} + \frac{1}{2}G_{H_2(g)} - G_X - G_{H_2O\ (l)} - k_B T \ln (10)pH - |e|u \tag{18}$$

$$\Delta G_2 = G_{X-O} + \frac{1}{2}G_{H_2(g)} - G_{X-OH} - k_B T \ln (10)pH - |e|u \tag{19}$$

$$\Delta G_3 = G_{X-OOH} + \frac{1}{2}G_{H_2(g)} - G_{X-O} - G_{H_2O\ (l)} - k_B T \ln (10)pH - |e|u \tag{20}$$

$$\Delta G_4 = G_{O_2} + G_X + \frac{1}{2}G_{H_2(g)} - G_{X-OOH} - k_B T \ln (10)pH - |e|u \tag{21}$$

$$\Delta G_1$$

$$= E_{X-OH,\ DFT} + \frac{1}{2}E_{H_2(g),\ DFT} - E_{X,\ DFT} - E_{H_2(} \tag{22}$$

$$- T\left(S_{X-OH} + \frac{1}{2}\ S_{H_2(g)} - S_X - S_{H_2O(l)}\right) - k_B T \ln ($$

$$\Delta G_2 = E_{X-O,\,DFT} + \frac{1}{2}E_{H_2(g),\,DFT} - E_{X-OH,\,DFT} + \left(E \right. \tag{23}$$
$$- k_B T \ln(10)pH - |e|u$$

$$\Delta G_3 = E_{X-OOH,\,DFT} + \frac{1}{2}E_{H_2(g),\,DFT} - E_{X-O,\,DFT} - E \tag{24}$$
$$- T\left(S_{X-OOH} + \frac{1}{2} S_{H_2(g)} - S_{X-O} - S_{H_2O(l)} \right) - k_B$$

$$\Delta G_4 = 4.92\,eV + E_{X,\,DFT} + 2\,E_{H_2O(l),DFT} - \frac{3}{2}E_{H_2(g),} \tag{25}$$
$$- T\left(S_X + 2\,S_{H_2O(l)} - \frac{3}{2}\,S_{H_2(g)} - S_{X-OOH} \right) - k_B$$

Finally, the catalytic performance of the different M-MOF-74 models was computed from the potential determining step (PDS), which represents the step with highest ΔG.[6] Its correlation with the theoretical overpotential is given by:

$$\eta_{theor} = \left(\frac{\Delta G_{PDS}}{e} \right) - 1.23\,V \tag{26}$$

3. Additional Gibbs energies

Table S2. ΔG (eV) for **A** and **B** considering ferromagnetic interwire and intrawire interactions.

Model	ΔG_1	ΔG_2	ΔG_3	ΔG_4	Overpotential (V)
A	1.40	1.89	0.94	0.69	0.66
B	0.89	2.34	0.80	0.89	1.11

Table S3. ΔG (eV) for **A** and **B** considering one explicit water molecule.

Model	ΔG_1	ΔG_2	ΔG_3	ΔG_4	Overpotential (V)
A	1.33	1.93	0.84	0.82	0.70
B	0.79	2.30	0.96	0.87	1.07

Table S4. ΔG (eV) for $\mathbf{C^A}$, $\mathbf{C^C}$, and $\mathbf{C^D}$ considering terminal **t** and bridge **b** sites.

Model	ΔG_1	ΔG_2	ΔG_3	ΔG_4	Overpotential (V)
$\mathbf{C^A}$-**t**	0.63	2.39	0.78	1.12	1.16
$\mathbf{C^A}$-**b**	0.63	2.00	1.33	0.96	0.77
$\mathbf{C^C}$-**t**	0.78	2.44	0.78	0.92	1.21
$\mathbf{C^C}$-**b**	0.80	2.27	1.04	0.81	1.04
$\mathbf{C^D}$-**t**	0.85	2.43	0.74	0.90	1.20
$\mathbf{C^D}$-**b**	0.84	2.25	0.98	0.85	1.02

4. Spin densities of periodic systems

Table S5. Spin densities of Fe and O atoms from the reactive centres of the OER intermediates obtained with pristine and defective periodic models and discussed in the main text.

Model	X	X-OH		X_1-O-X_2			X_1-OOH-X_2		
	Fe	Fe	O	Fe_1	O	Fe_2	Fe_1	O	Fe_2
B	-3.84	-4.42	-0.21	-3.96	-0.20		-4.33	-0.25	
$\mathbf{C^B}$-**t**	3.84	4.42	0.20	4.03	0.18		4.34	0.24	
$\mathbf{C^B}$-**b**	3.84	4.42	0.20	4.34	0.20	3.79	4.40	0.20	3.85
D-t	3.84	4.41	0.21	4.13	0.25		4.32	0.25	
D-b	3.84	4.41	0.21	4.35	0.27	3.85	4.40	0.12	3.84
D-b'	3.84	4.41	0.21	4.40	0.21	3.86	4.40	0.10	3.84

5. Cluster calculations

We prepared a finite-size 88-atom cluster model[7] of Fe-MOF-74 from the PBE+U optimized periodic structure. This model contains six DOBDC linkers and a metal wire with three five-coordinate Fe(II) cations. In order to ensure the neutrality of the system, hydrogen atoms were employed to (i) replace the carboxylate (COO⁻) and oxido (O⁻) functional groups of the DOBDC that are negatively charged and non-coordinated to Fe and to (ii) cap three COO⁻ groups coordinated to the metal wire. The resulting neutral cluster contains a central Fe with totally equivalent chemical environment to the metals of the crystal structure and two peripheral metals with slightly modified coordination (Fig. S3). This cluster model was taken as starting point to compute the four intermediates involved in the OER. During the relaxation of the structures, all carbon atoms of the DOBDC linker but the ones belonging to COO⁻ groups were kept frozen with the aim of preserving the structural and electronic features of the Fe-MOF-74 crystal structure.
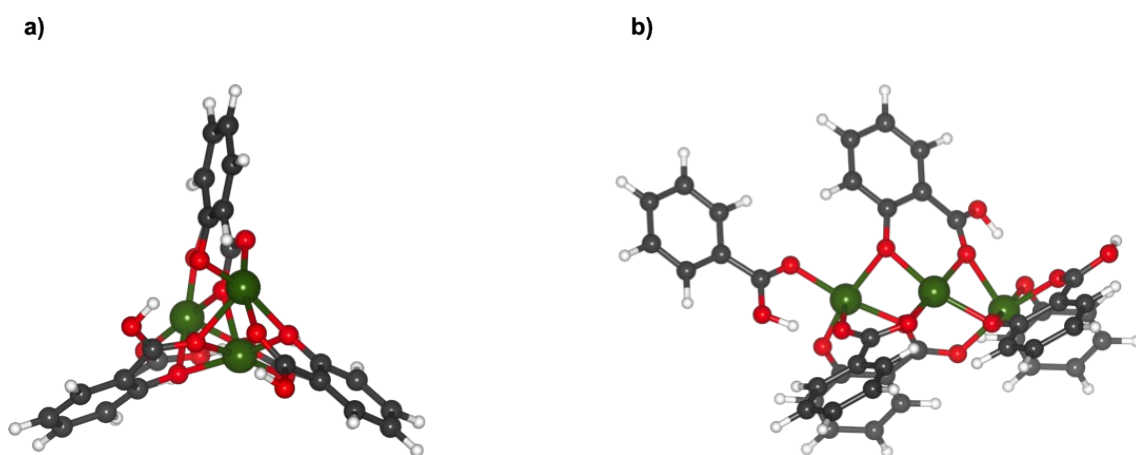
a)   b)

Fig. S3 a) Top view and b) side view of cluster model of Fe-MOF-74. Atom legend: Fe (green), O (red), C (grey), and H (white).

The optimizations of the intermediates were carried out using DFT employing several exchange-correlation functionals with an ultrafine grid as implemented in Gaussian09[8]. A General Gradient Approximation (GGA) based density functional (PBE[9,10]), a meta-GGA (M06-L[11]) and five hybrids with different percentage of nonlocal Hartree–Fock exchange (HSE03-13[12], B3LYP-15[13], B3LYP[14,15,16], HSE03[17,18], and PBE0[19]). D3 empirical dispersion[20] was included in all calculations but the ones carried out with M06-L density functionals. The 6-31G (d,p) basis sets[21,22,23] were used for all atoms and diffusion functions[22,23] were added for O atoms. The core electrons of Fe atoms were described with the scalar-relativistic Stuttgart–Dresden SDD pseudopotential and the outer ones with its associated double-ζ basis set.[24] All geometry relaxations were performed in gas phase and the solvation energy of H_2O was computed in water using the SMD model.[25]

The analytical vibrational frequencies were computed (i) to confirm that all intermediates are minima in the potential energy surface and (ii) to calculate their corresponding Gibbs energies. The thermodynamics of OER were computed following the computational hydrogen electrode method as explained in section 2.

Table S6. Spin densities of Fe and O atoms from OER intermediates obtained with the cluster model of Fe-MOF-74 employing different density functionals.

DF	X^a	X	X-OH		X-O		X-OOH	
		Fe	Fe	O	Fe	O	Fe	O
PBE+U[b]	0	-3.84	-4.42	-0.21	-3.96	-0.20	-4.33	-0.25
PBE	0	3.79	4.00	0.32	2.90	0.55	3.93	0.34
M06-L	0	3.87	4.04	0.33	3.03	0.48	3.97	0.32
HSE03-13	13	3.87	4.22	0.36	3.28	0.53	4.13	0.36
B3LYP-15	15	3.82	4.19	0.37	3.23	0.56	4.11	0.36
B3LYP	20	3.84	4.23	0.35	3.31	0.50	4.16	0.36
HSE03	25	3.90	4.33	0.36	3.49	0.36	4.25	0.35
PBE0	25	3.90	4.32	0.34	3.47	0.37	4.24	0.35

[a] Percentage of nonlocal Hartree–Fock exact exchange.
[b] Spin densities from the periodic model.

Table S7 ΔG (eV) of the cluster model of Fe-MOF-74 employing different density functionals.

DF	χ^a	ΔG_1	ΔG_2	ΔG_3	ΔG_4	Overpotential (V)
PBE+U[b]	0	0.87	2.40	0.79	0.86	1.17
PBE	0	0.20	1.30	1.85	1.57	0.62
M06-L[c]	0	0.22	1.80	1.48	1.42	0.57
HSE03-13	13	0.57	1.84	1.50	1.01	0.61
B3LYP-15	15	0.54	1.82	1.51	1.05	0.59
B3LYP	20	0.66	2.03	1.36	0.87	0.80
HSE03	25	0.80	2.35	1.16	0.61	1.12
PBE0	25	0.82	2.38	1.13	0.59	1.15

[a] Percentage of nonlocal Hartree–Fock exact exchange.
[b] Gibbs energies from the periodic model.
[c] **X-O** and **X-OOH** contain one imaginary frequency that was not possible to remove.

6. References

1. P. D. C. Dietzel, Y. Morita, R. Blom and H. Fjellvåg, *Angew. Chem. Int. Ed.,* 2005, **44**, 6354.

2. V. Tripkovic, E. Skúlason, S. Siahrostami, J. K. Nørskov and J. Rossmeisl, *Electrochim. Acta* 2010, **55**, 7975.

3. D. R. Lide, Handbook of Chemistry and Physics. 84th edition, CRC Press, 2003.

4. J. K. Nørskov, J. Rossmeisl, A. Logadotirr, L. Lindqvist, J. R. Kitchin, T. Bligaard and H. Jónsson, *J. Phys. Chem. B*, 2004, **108**, 17886.

5. M. Garcia-Ratés and N. López, *J. Chem. Theory Comput.*, 2016, **12**, 1331.

6. l. C. Man, H. Su, F. Calle-Vallejo, H. A. Hansen, J. I. Martínez, N. G. Inoglu, J. Kitchin, T. F. Jaramillo, J. K. Nørskov and J. Rossmeisl, *ChemCatChem*, 2011, **3**, 1159.

7. P. Verma, X. Xu and D. G. Truhlar, *J. Phys. Chem. C* **2013**, *117*, 12648.

8. Gaussian 09, Revision A-02, M. J. Frisch, G. W. Trucks, H. B. Schlegel, G. E. Scuseria, M. A. Robb, J. R. Cheeseman, G. Scalmani, V. Barone, B. Mennucci, G. A. Petersson, H. Nakatsuji, M. Caricato, X. Li, H. P. Hratchian, A. F. Izmaylov, J. Bloino, G. Zheng, J. L. Sonnenberg, M. Hada, M. Ehara, K. Toyota, R. Fukuda, J. Hasegawa, M. Ishida, T. Nakajima, Y. Honda, O. Kitao, H. Nakai, T. Vreven, J. A. Montgomery, Jr., J. E. Peralta, F. Ogliaro, M. Bearpark, J. J. Heyd, E. Brothers, K. N. Kudin, V. N. Staroverov, R. Kobayashi, J. Normand, K. Raghavachari, A. Rendell, J. C. Burant, S. S. Iyengar, J. Tomasi, M. Cossi, N. Rega, J. M. Millam, M. Klene, J. E. Knox, J. B. Cross, V. Bakken, C. Adamo, J. Jaramillo, R. Gomperts, R. E. Stratmann, O. Yazyev, A. J. Austin, R. Cammi, C. Pomelli, J. W. Ochterski, R. L. Martin, K. Morokuma, V. G. Zakrzewski, G. A. Voth, P. Salvador, J. J. Dannenberg, S. Dapprich, A. D. Daniels, Ö. Farkas, J. B. Foresman, J. V. Ortiz, J. Cioslowski, and D. J. Fox, Gaussian Inc., Wallingford CT, 2016.

9. J. P. Perdew, K. Burke and M. Ernzerhof, *Phys. Rev. Lett.*, 1996, **77**, 3865.

10. J. P. Perdew, K. Burke and M. Ernzerhof, *Phys. Rev. Lett.*, 1997, **78**, 1396.

11. Y. Zhao and D. G. Truhlar, *J. Chem. Phys.*, 2006, **125**, 194101.

12. F. S. Hegner, F. S. D. Cardenas-Morcoso, S. Giménez, N. López, and J. R. Galan-Mascarós, *ChemSusChem*, 2017, **10**, 4552.

13. M. Reiher, O. Salomon and A. Hess, *Theor. Chem. Acc.*, 2001, **102**, 48.

14. C. Lee, W. Yang and R. G. Parr, *Phys. Rev. B.*, 1988, **37**, 785.

15. A. D. Becke, *J. Chem. Phys.*, 1993, **98**, 5648.

16. P. Stephens, F. J. Devlin, C. F. Chabalowski and M. J. Frisch, *J. Phys. Chem.*, 1994, **98**, 11623.

17. J. Heyd, G. E. Scuseria and M. Ernzerhof, *J. Chem. Phys.*, 2003, **118**, 8207.

18. J. Heyd, G. E. Scuseria and M. Ernzerhof, *J. Chem. Phys.*, 2006, **124**, 219906.

19. C. Adamo and V.Barone, *J. Chem. Phys.,* 1999, **110**, 6158.

20. S. Grimme, J. Antony, S. Ehrlich and H. A. Krieg, *J. Chem. Phys.*, 2010, **132**, 154104.

21. R. Ditchfield, W. Hehre and J. A. Pople, *J. Chem. Phys.*, 1971, **54**, 724.

22. P. C. Hariharan and J. A. Pople, 1973, **28**, 213.

23. W. Hehre, R. Ditchfield and J. A. Pople, *J. Chem. Phys.,* 1972, **56**, 2257.

24. M. Dolg, U. Wedig, H. Stoll and H. Preuss, *J. Phys. Chem.,* 1987, **86**, 866.

25. A. V. Marenich, C. J. Cramer and D. G. Truhlar, *J. Phys. Chem. B.*, 2009, **113**, 6378.